Journal of Quantitative Spectroscopy & Radiative Transfer 196 (2017) 78–86

Contents lists available at ScienceDirect

Journal of Quantitative Spectroscopy & Radiative Transfer

journal homepage: www.elsevier.com/locate/jqsrt

Accurate modeling of the diagnostic 118-GHz oxygen line for remote sensing of the atmosphere

M.A. Koshelev [a,*], T. Delahaye [b], E.A. Serov [a], I.N. Vilkov [a], C. Boulet [c], M.Yu. Tretyakov [a]

[a] Institute of Applied Physics RAS, 46 Ul'yanov street, 603950 Nizhny Novgorod, Russia
[b] Laboratoire de Météorologie Dynamique/IPSL, CNRS, Ecole polytechnique, Université Paris-Saclay, 91128 Palaiseau, France
[c] Institut des Sciences Moléculaires d'Orsay (ISMO), CNRS, Univ. Paris-Sud, Université Paris-Saclay, Bât. 350, Campus d'Orsay F-91405, France

ARTICLE INFO

Article history:
Received 14 February 2017
Received in revised form
23 March 2017
Accepted 30 March 2017
Available online 4 April 2017

Keywords:
oxygen
fine structure lines
collision relaxation
pressure broadening
speed dependence
line mixing
atmospheric applications

ABSTRACT

We report the results of laboratory investigations of the shape of the diagnostic atmospheric N = 1-oxygen line performed over a very wide range of pressures from 0.4 to 1000 Torr using two principally different spectrometers having complementary abilities. A spectrometer with a radio-acoustic detector of absorption was used for recording low pressure spectra spanning the 0.4–2 Torr range, and high pressure data from 250 to 1000 Torr were registered by a resonator spectrometer. The sensitivity of both instruments was improved significantly which allowed us to obtain signal-to-noise ratio at spectra recordings of the order of a few thousands. The spectra analysis enabled the first manifestation of the speed-dependence of the collision cross section of the line, along with considerable refinement of other parameters, including pressure broadening, intensity and line-mixing. The results are of primary importance for atmospheric applications.

1. Introduction

The present day methods of remote sensing demand high accuracy spectroscopic information about the diagnostic lines employed. The requirements for information accuracy are becoming increasingly more stringent. Line intensity and line width are known to be the most crucial parameters affecting accuracy of the retrieved atmospheric data. Another important issue is that a single measurement of a parameter cannot ensure the declared (usually statistic) uncertainty due to possible systematic errors (see, e.g., Figs. 15–17 in Ref. [1]). So, reliable information can be obtained only from the multiple studies of a target line by different spectroscopic laboratory techniques in a wide range of conditions.

A single fine structure oxygen line near 118 GHz is an important diagnostic line that serves in remote sensing as a “temperature and pressure sensor” (see, e.g. [2,3]). This line has been a subject of a large number of studies [4–13], including a series of our works [14–20]. We believe that the results of our studies provide the most accurate to date experimental values of line intensity [18], pressure broadening [19,20] and mixing coefficients [18] and their temperature dependences [20]. In the aforementioned studies of the 118-GHz line we used spectrometers having different measurement principles, significantly different working pressures and complementary abilities. Coincidence of some parameters (e.g., pressure broadening coefficients) measured by different methods allowed us to claim high reliability of the data obtained in those studies. The main limitation of those data concerns the use of the basic line shape models for fitting experimental spectra: the Voigt and Rosenkranz profiles respectively for low and high pressures. Indeed, it is well known [21] that in most cases these simple models fail to reproduce the experimental line profile recorded with a sufficiently high signal-to-noise ratio (SNR). Thus, deviation of the Voigt profile from the experimental one is typically about 1–2% of the peak absorption (see, for example [22–25],) reaching up to 8–9% [26,27] limiting accuracy of atmospheric profile modeling.

Achieving better accuracy requires taking into account first of all the dependence of collisional width and shift on the speed of absorbing molecules [28] called the speed-dependence (SD) or ‘wind’ effect, and velocity-changing collisions causing the Dicke narrowing [29]. For the lines of millimeter and submillimeter wavelength range, where Doppler broadening is relatively small, the SD-effect has been shown [22] to be the major cause of deviation of the experimental line shape from the Voigt profile, even at relatively low pressures corresponding to the conditions of the upper stratosphere. For the oxygen fine structure lines this effect has never been studied before and has not been taken into account in the models of atmospheric absorption of radiation by oxygen.

* Corresponding author.
E-mail address: koma@ipfran.ru (M.A. Koshelev).
URL: http://www.mwl.sci-nnov.ru (M.A. Koshelev).

http://dx.doi.org/10.1016/j.jqsrt.2017.03.043
0022-4073/

However, even thorough modeling of the shape of the 60-GHz oxygen band formed by a large number of fine structure lines demonstrates [30] the difference of the calculated profiles from the experimental spectra by about 1–2%. This difference may be a result of neglecting the SD-effect in the model. Analysis of oxygen line shape at high enough pressures (hundreds of Torr) demands allowance for the cumulative effect of the SD and the line mixing that impedes such studies.

In this paper we report the results of laboratory investigations of the shape of the 118-GHz oxygen line performed over a very wide range of pressures (0.4–1000 Torr) using two principally different spectrometers having complementary abilities. The spectrometer with radio-acoustic detector [31] was used to record low pressure spectra spanning the 0.4–2 Torr range, and high pressure data from 250 to 1000 Torr were recorded with a resonator spectrometer [32]. The considerably improved sensitivity of both instruments allowed us to obtain signal-to-noise ratio at spectra recordings of the order of a few thousands. The spectra analysis enabled the first manifestation of the speed-dependence of collisional broadening of the line, along with considerable refinement of other parameters of the line, including collisional broadening, line-mixing and integrated intensity.

2. Low pressure experiment using RAD spectrometer

A spectrometer with a backward-wave oscillator (BWO) and a radio-acoustic detector of absorption (RAD spectrometer) [31] was used for studying the 118-GHz oxygen line in the 0.4–2 Torr pressure range. The spectrometer and the measurement method are similar to those used in our earlier studies [19,20,33], so we present here only their brief description and main changes in the setup and method. A copper gas cell ($\sim$10 cm long, $\sim$1.5 cm in diameter) was placed inside a double shield made of annealed permalloy to avoid distortion of the shape of the magnetic-dipole oxygen line by external magnetic fields. The cell was permanently connected with the Julabo FP-50 HE thermostat that provides stable temperature of a coolant inside the thermostat within $\pm$0.01°C around the chosen value of 23.7°C. The cell and both shields were additionally packed into a heat-isolating material minimizing temperature gradients and drifts. Four copper temperature sensors were mounted on the cell surface and allowed temperature control of the gas sample inside the cell to an accuracy of $\pm$0.5°C. It should be noted that for the current room-T study no gradients and drifts of the cell temperature were revealed within the T-sensors accuracy. Gas pressure in the cell was permanently monitored using a 10-Torr range MKS Baratron (Type 626B) gauge having a declared accuracy of 0.25% of reading.

In our previous studies of the oxygen fine structure lines using RAD spectrometer the signal-to-noise ratio of the recorded spectra was about a few hundreds for 1 s integration time constant [19,20,33]. However, this is almost an order of magnitude less than the SNR required for observation and study of the SD effect. To achieve the required SNR, some components and parameters of the previous RAD spectrometer were modified. In particular, for reducing the influence of external acoustic and mechanical noise the cell was weighted by about twenty five kilograms by the small lead balls 3-mm in diameter (initial cell weight was about 2.5 kg). This allowed a fivefold increase of the SNR of the experimental spectra. Analysis of the line recordings obtained at different amplitude modulation frequencies in the 70–290 Hz range revealed a possibility of further SNR improvement. The frequency should be outside unfavorable intervals that occur probably because of mechanical resonances in the setup elements (table, vacuum system, etc.). The use of the modulation frequency of 80 Hz instead of the previously used 180 Hz give a 25% increase of SNR.

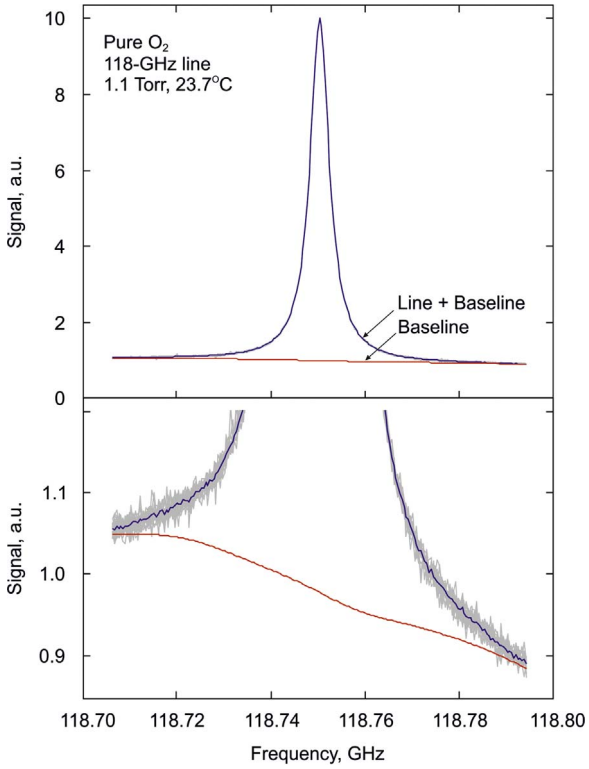

Fig. 1. (Color online) Experimental spectra of pure oxygen near 118.75 GHz. The lower plot is a zoomed-in part of the upper plot. Twenty spectra recorded at 1.1 Torr of pure oxygen are shown by grey. The blue curve is the result of their averaging. The red curve shows the baseline recorded for the same conditions with 1.1 Torr of pure nitrogen.

Finally, high stability of radiation parameters (frequency and power) and experimental conditions (room and cell temperature, pressure in the cell) allowed averaging a large number of repeated experimental recordings for each chosen pressure for achieving SNR of a few thousands. The number of averaged line recordings varied from 40 for lower pressure (lower sensitivity of the acoustic cell) down to 20 for higher pressures. An example of averaging twenty experimental spectra is shown in Fig. 1.

At the next step of experimental spectra treatment, the instrumental baseline was taken into account. The baseline arises from absorption of the radiation by the cell elements providing secondary gas heating and thus producing a microphone signal synchronous with modulation. Similarly to our previous studies the baseline signal was recorded at the same configuration of the waveguide line of the spectrometer and the pressure of nitrogen (negligibly absorbing in mm/submm range under these conditions) in the cell same as for oxygen spectra recording (see Fig. 1). Experimental baseline was subtracted from the sample spectra and the obtained spectra were then used for the line shape analysis.

3. High pressure experiment using resonator spectrometer

A modified version of the resonator spectrometer was employed for studying the shape of the 118-GHz line in the pressure range of 250–1000 Torr. A detailed description of the spectrometer and measurement method used in our earlier studies of the oxygen fine structure lines [16,18,33] is given in Refs [32,34]. The block diagram of the modified spectrometer is presented in Fig. 2.

The gas absorption measurement is based on determining the Fabry–Perot resonator Q-factor. The latter can be found as a ratio of eigenfrequency and resonance curve width, leading to the following

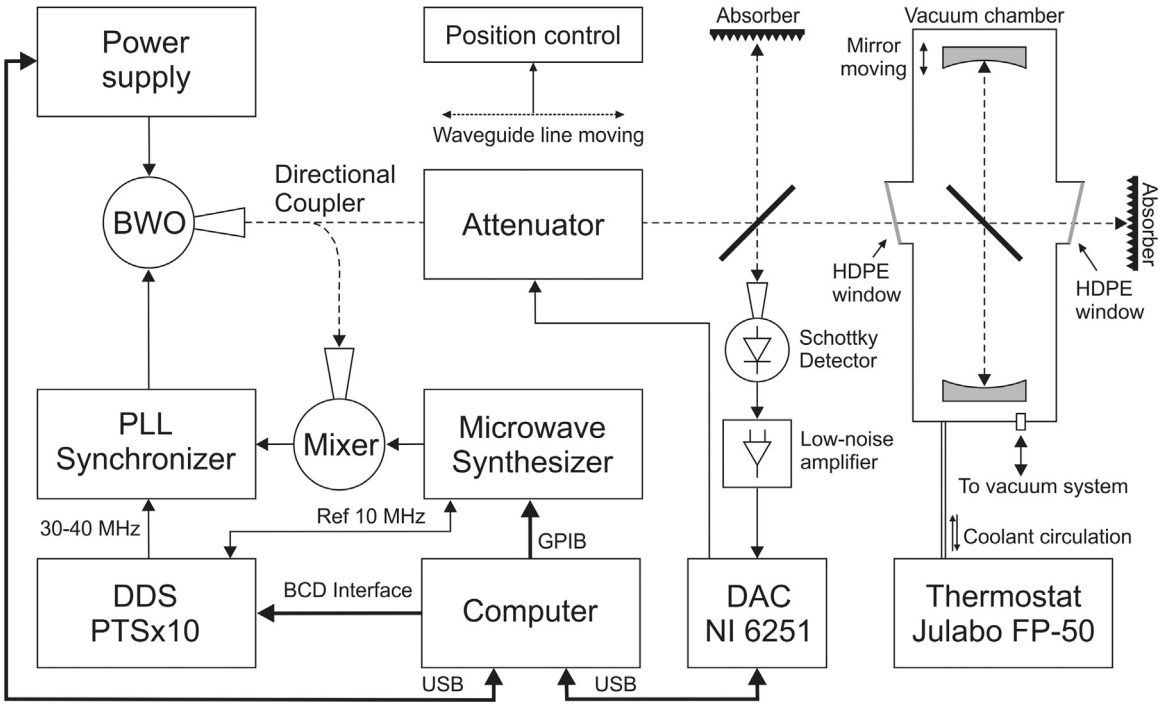

Fig. 2. Block diagram of resonator spectrometer.

formula for gas absorption coefficient α [35]:

$$\alpha = \frac{2\pi}{c}\left(\Delta f - \Delta f_0\right), \tag{1}$$

where c is the speed of light in the studied gas, Δf and Δf_0 are, respectively, the widths of the resonance curve of the resonator filled with the studied gas and with a non-absorbing gas (we used Ar in the present study).

BWO tubes (OB-76 in the current study) are used as coherent continuous wave radiation sources of the spectrometer. The sources are equipped with a system of precise digital frequency stabilization and control based on a phase-locked loop (PLL) system. The system includes two synthesizers: a microwave (MW) synthesizer (Agilent E8257D, 100 kHz – 40 GHz) defining the central frequency of BWO and a direct digital synthesizer (DDS) PTS × 10, 30–40 MHz range for fast step-by-step sweeping of the BWO frequency around the chosen central frequency with 2-μs switching time and without loss of the oscillation phase. It is the principal condition for work with a resonator in frequency domain, in particular for fast recording of a resonance curve. It is worth noting that the previously used homemade DDS based on AD9850 microcircuit in combination with a specialized processor allowed only 58-μs time between frequency switching [36]. For the current version of the resonator spectrometer, a 40-μs switching time was found experimentally as a compromise between signal-to-noise ratio, time of recording and distortion of the resonance curve. A further decrease of switching time is limited by the bandwidth of the available detector signal amplifier.

Sample spectra and baseline are recorded at frequencies corresponding to eigenmodes of the Fabry-Perot resonator. The BWO frequency is changed from one eigenmode to another one by changing the MW synthesizer frequency and BWO control voltage. The corresponding list of the resonator eigenfrequencies for the current configuration under certain experimental conditions and the BWO control voltages was prepared for the required frequency range. The BWO frequency change and resonance curve recording occur in fully automatic regime. The attenuator control in the quasi-optical line is also automatic, which maintains the radiation power at a fixed level minimizing the influence of detector characteristic nonlinearity. The upgrade of the systems of frequency and power control and data acquisition allowed more than tenfold gain in the time of the spectra recording in comparison with the previous version of the spectrometer. Thus, recording of oxygen spectrum consisting of about 100 points previously lasted about 130 minutes, and now it takes about 12 minutes.

Temperature was permanently controlled by eight copper thermistors (the stated accuracy of ± 0.5°C) placed on resonator elements and inside the cavity. For decreasing temperature gradients, the resonator was placed inside the copper case (wall thickness is about 5 mm) permanently connected with the thermostat Julabo FP-50 HE. It is stated by the manufacturer that the thermostat allows temperature control within the -50°C to 200°C range with the internal bath stability of ± 0.01°C. The current study was carried out at room temperature and no gradients or temperature drifts were revealed within the stated accuracy of T-sensors.

The resonator with the copper case was placed inside the stainless steel vacuum chamber of about 200 l volume connected with a vacuum system for pumping and gas puffing. A dry scroll vacuum pump (Anest Iwata DVSL-500C) and a pumping station Pfeiffer Hi-Cube 80 with turbo pump were employed for chamber degasing. Pressure inside the chamber was controlled by two capacitance manometers: Pfeiffer CCR361 (1000-Torr range) and CCR362 (100-Torr range) with 0.2% stated uncertainty of measurement.

For the current study we used a Fabry-Perot resonator with two spherical mirrors having a diameter of 12 cm and a curvature radius of about 49 cm. The distance between the mirrors was about 41.6 cm and could be smoothly varied within 30-mm interval. A 10 μm thick teflon film placed at 45° to the resonator axis was used for coupling the resonator with the radiation source. The finesse of the empty resonator was about 2000 in the studied frequency interval. Radiation coming from the resonator was detected by a point contact diode based detector.

The method of sample absorption measurement is similar to the one used in our previous studies (see, e.g [16,33,35].). Four oxygen pressures (250, 500, 750 and 1000 Torr) were chosen for the study of the 118-GHz line shape.

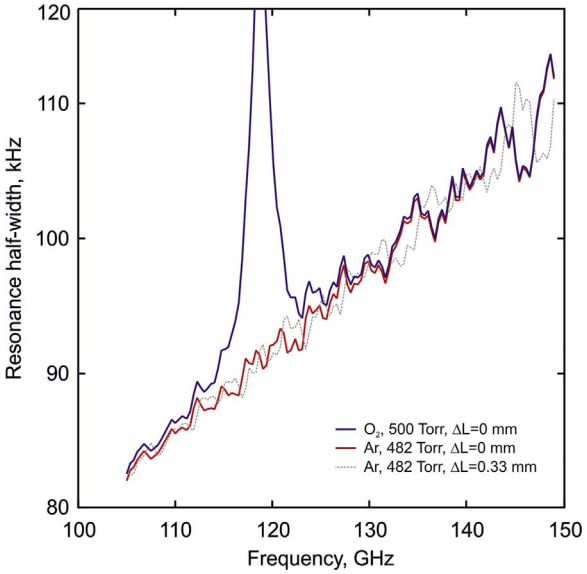

Fig. 3. (Color online) Frequency dependence of the resonance half-width obtained at 500 Torr of oxygen (blue) and 482 Torr of argon (red and grey). The blue and red curves were obtained at the same relative positions of the waveguide line and the resonator while for the grey curve recording the waveguide line was moved by 0.33 mm. The temperature was 23.5°C.

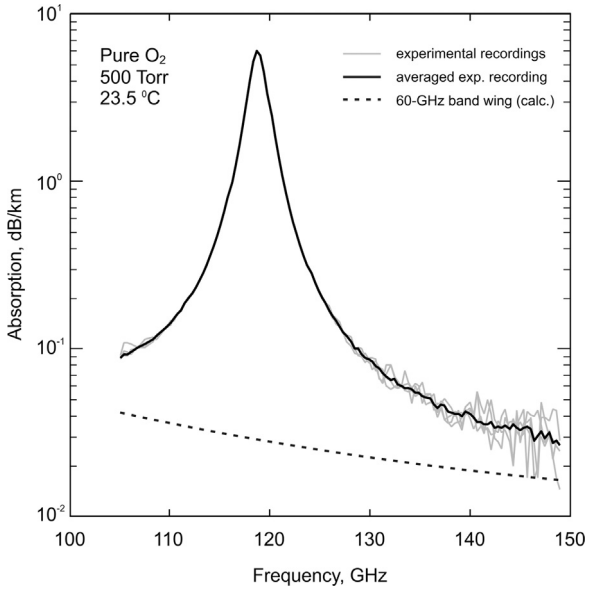

Fig. 4. Four recordings of pure oxygen spectrum at 500 Torr and 23.5°C are shown by grey color. The black curve is the averaged spectra. Absorption in the wing of the 60-GHz band calculated using MPM (version for pure oxygen) [33] is shown by the dashed line. Note logarithmic scale of the absorption axis.

For each chosen pressure, the experiment started with recording oxygen (99.995% purity) spectrum. Then the resonator chamber was evacuated and filled with argon (99.9%) at the pressure supplying the same list of eigenfrequencies without mechanical tuning of the distance between the mirrors. The latter allows maintaining the same pattern of the radiation standing waves both in the waveguide line and in the resonator which is manifested as a quasi-periodic behavior in both baseline and sample spectra recordings illustrated in Fig. 3. It should be noted that changing the position of the resonator relative to the radiation source as well as changing the mirror position entails change of the pattern of standing waves and corresponding systematic errors of measured resonance widths (see Fig. 3) limiting absorption measurement accuracy. Temperature variations in the lab during the experiment can also influence the standing waves worsening the reproducibility of the baseline. Use of active laboratory conditioning and heat-insulation of the waveguide line from ambient air allowed us to keep the whole setup temperature stable within ± 0.3°C in the course of measurement (a few hours).

At the next step we moved the radiation source together with the related waveguide line along its axis relative to the resonator by about 0.3 mm (approximately $\lambda/8$, λ is wavelength) and repeated the baseline recording since the resonator was already filled with Ar. Then the chamber was degassed and filled with O_2 exactly at the pressure of the first measurement and the sample spectra recording was repeated. In total, for each oxygen pressure the data sets (including sample spectra and corresponding baseline) were sequentially recorded at four different positions of the resonator and source. Stable and well controlled conditions of both the setup and the sample enabled significant gain in signal-to-noise ratio after averaging of the obtained spectra (see Fig. 4). This method of averaging of the spectra recorded at different positions of the resonator and the source allowed decreasing both statistical noise and systematically outlying points related to the small changes of the baseline in O_2 and Ar. The latter may be caused, for example, by pressure difference in spectra and baseline recording which lead to small deviations in the position of the chamber windows made of high-density polyethylene (10 mm thick) and corresponding small changes in the standing wave pattern.

More points are required for the line recording within a fixed frequency interval at lower pressures because the line becomes narrower. For the resonator spectrometer, the frequency list and the corresponding number of points are determined primarily by the distance between the mirrors. So, to achieve a larger number of points around the line center without essentially increasing the size of the resonator and the chamber, line recording at each pressure was performed at two (at 500 Torr) or three (at 250 Torr) positions of the upper mirror differing from each other by $\lambda_0/4$ or $\lambda_0/6$, respectively (λ_0 is wavelength at the line center). At each mirror position, line recording was performed following the procedure described above: sample and baseline were recorded at four different positions of the resonator and the source. Then the mirror position was changed and the spectrum recording in the vicinity of the line center was repeated. This procedure allowed avoiding losses of the informative part of the spectra in the vicinity of the line center at low (for this setup) pressures.

4. Line shape models for oxygen fine structure lines

As the pressure range and collisional regime are strongly different in the two experimental setups described above, the analysis of the obtained spectra was performed considering two types of line shape models. For the high pressure spectra recorded using the resonator spectrometer, the Doppler effect becomes totally negligible compared to the collisional effects and the line width becomes comparable with its central frequency, so that we can consider the usual Van Vleck-Weisshopf (VVW) profile [37]. High signal-to-noise ratio of the recorded spectra (a few thousands), requires refining this simple line profile to consider the speed dependence of the collisional relaxation rate in the model, leading to the so-called quadratic Speed Dependent Van Vleck-Weisskopf (qSDVVW) line shape described by the following expression

$$qSDVVW(\omega-\omega_0,\Delta(\nu),\Gamma(\nu))=\frac{1}{\pi}\left(\frac{\omega}{\omega_0}\right)^2 Re\left\{\int f_{MB}(\nu)\left[\frac{-i}{\omega-\omega_0-\Delta(\nu)-i\Gamma(\nu)}-\frac{i}{\omega+\omega_0+\Delta(\nu)-i\Gamma(\nu)}\right]d\nu\right\}. \quad (2)$$

where ω and ω_0 are angular frequency and line center, respectively; $f_{MB}(\nu)$ is the Maxwell-Boltzmann distribution. Speed dependences of the collisional half-width $\Gamma(\nu)$ and shift $\Delta(\nu)$ are modeled by the quadratic law proposed by Rohart et al. [38,39]:

$$\Gamma(\nu)+i\Delta(\nu)=\Gamma_0+i\Delta_0+(\Gamma_2+i\Delta_2)\left[\left(\frac{\nu}{\tilde{\nu}}\right)^2-\frac{3}{2}\right], \quad (3)$$

$\tilde{\nu}=\sqrt{2k_BT/m}$ is the most probable speed of an absorbing molecule of mass m.

Because of the line mixing effect of the 118-GHz line with the other fine-structure lines located near 60 GHz, the resulting intensity of the band cannot be represented as a simple sum of isolated line profiles as in Eq. (2). Instead, a model accounting for the line mixing effect in the first-order Rozenkranz approximation [40] was considered as

$$qSDVVWLM(\omega-\omega_0,\Delta(\nu),\Gamma(\nu),Y)=Re\left\{(1+iY)\cdot qSDVVW(\omega-\omega_0,\Delta(\nu),\Gamma(\nu))\right\}. \quad (4)$$

The contribution of the second-order terms of the Rozenkranz approximation [41] was estimated to be very small for this line with respect to the available signal-to-noise ratio of the recordings. Therefore, parameters of the second-order line-mixing approximation were not adjusted in the analysis but held fixed to their estimated value determined from MPM (Millimeter-wave Propagation Model) calculations [41] taking into account the concentration of absorbing molecules. The contribution of these terms was added at each step of the fitting procedure to the simulated spectra (see Section 4 for details). The following expression was used for modeling the absorption observed at high pressures

$$M(\omega)=a_0\cdot qSDVVWLM(\omega-\omega_0,\Gamma_0,\Gamma_2,Y)+a_1+a_2(\omega-\omega_0)+a_3(\omega-\omega_0)^2 \quad (5)$$

where $a_{0\ldots3}$ are variable parameters allowing for the line total area (a_0) and baseline ($a_{1\ldots3}$) adjustments. The Rosenkranz profile (labeled further in the text as VVWLM) which can be obtained from Eq. (4) assuming $\Gamma_2=\Delta_2=0$ was also used in the high pressure model (5) for comparison with the advanced profile (4).

Concerning the low pressure spectra obtained using a RAD spectrometer, the line width is rather small compared to the central frequency but the Doppler effect is no more negligible compared to collisional effects and must be included in the considered line shape model. Therefore, the so-called quadratic Speed-dependent Voigt profile (qSDVP) was employed:

$$qSDVP(\omega-\omega_0,\Delta(\nu),\Gamma(\nu))=\frac{1}{\pi}Re\left\{\int\frac{-i\cdot f_{MB}(\nu)}{\omega-\omega_0-\vec{k}\cdot\vec{\nu}-\Delta(\nu)-i\Gamma(\nu)}d\nu\right\} \quad (6)$$

Finally, the line absorption for low pressures data was modeled by the expression

$$M(\omega)=a_0(1+a_4(\omega-\omega_0))\cdot qSDVP(\omega-\omega_0,\Gamma_0,\Gamma_2)+a_1+a_2(\omega-\omega_0)+a_3(\omega-\omega_0)^2 \quad (7)$$

where $a_{0\ldots4}$ are fitted parameters modeling the spectrometer baseline (details can be found in Ref. [31]). The Voigt profile (VP) was also used in the low pressure model (7) for comparison with the advanced profile (6).

5. Data analysis

Both experimental (RAD and resonator spectrometers) data sets were treated separately using two different approaches. The first one is the multispectrum fitting in which model function was fitted simultaneously to all recorded spectra. This approach allows constraining the linear pressure dependence of line shape parameters and decreasing the numerical correlation between these parameters. The fitting procedure was realized using a recently developed code [42] which provides adjustable parameters related to each spectrum considered (surface, baseline) and to each spectral line (lineshape-dependent parameters such as collisional broadening, shifting, line-mixing…). A particular feature of this code is that we can calculate complex line profiles, such as the HTp [43] or qSDVP, along with line mixing through the first-order approximation.

The second method of data analysis is traditional line-by-line approach which implies separate adjusting of each parameter of the line at a given pressure. The pressure-independent coefficients were then retrieved by linear approximation of the line parameters obtained from the fit. The results of these analyses for both sets of data are discussed and compared in what follows.

Residuals of multispectrum and line-by-line fits of the model function (VP and qSDVP) to the low pressure (RAD) data are shown in Fig. 5. Note that the normalized frequency scales make easy intercomparison of all residuals. First of all we note that the use of the Voigt profile neglecting the speed-dependence effect resulted in the typical w-shape discrepancy in the residuals. Use of the qSDVP-based model function gave better description of the experimental spectra for both multifit and line-by-line fit. However, it is apparent that the multispectrum fit exhibits a small peak centered at f_0 in residuals at lower and higher pressures, whereas this structure is totally vanished in line-by-line fits. The most probable reason of this is the high constraint on the pressure linearity of the parameters imposed by the multispectrum fitting procedure. All pressure uncertainties are thus contained in the fit residuals, whereas in the case of line-by-line analysis these uncertainties are converted into values of line parameters entailing scattering of the points from linear dependence. It is worth noting, that small variation of pressure values within the stated uncertainty of the pressure gauge allowed vanishing systematic variations in the residuals. No clear structure is seen in the line-by-line residuals meaning that the considered qSDVP model is appropriate for analysis of our spectra.

The resonator spectrometer (high pressures) data and treatment results are shown in Fig. 6. Again, it is seen that neglecting the speed dependent effect (VVWLM profile) causes systematic distortion in the fit residuals, while the qSDVVWLM model enables a very good representation of the measured spectra (SNR is about 3000) with residuals of the order of 0.3% from the line amplitude or better in all cases. Similarly, to the low pressure data, the multifit approach revealed small distortion in the residuals. However, its manifestation is less evident for the high pressure spectra that might mean less uncertainty in pressure measurement. As mentioned in the previous section, the line-mixing contribution was fitted through the adjustment of the first-order approximation parameter Y. Evaluations of the second order terms contribution (Fig. 6) from MPM calculations [41] showed that even at the highest pressure (i.e. 1000 Torr) the influence of the 2nd order approximation was very small. For this reason, we didn't adjust the second order parameters

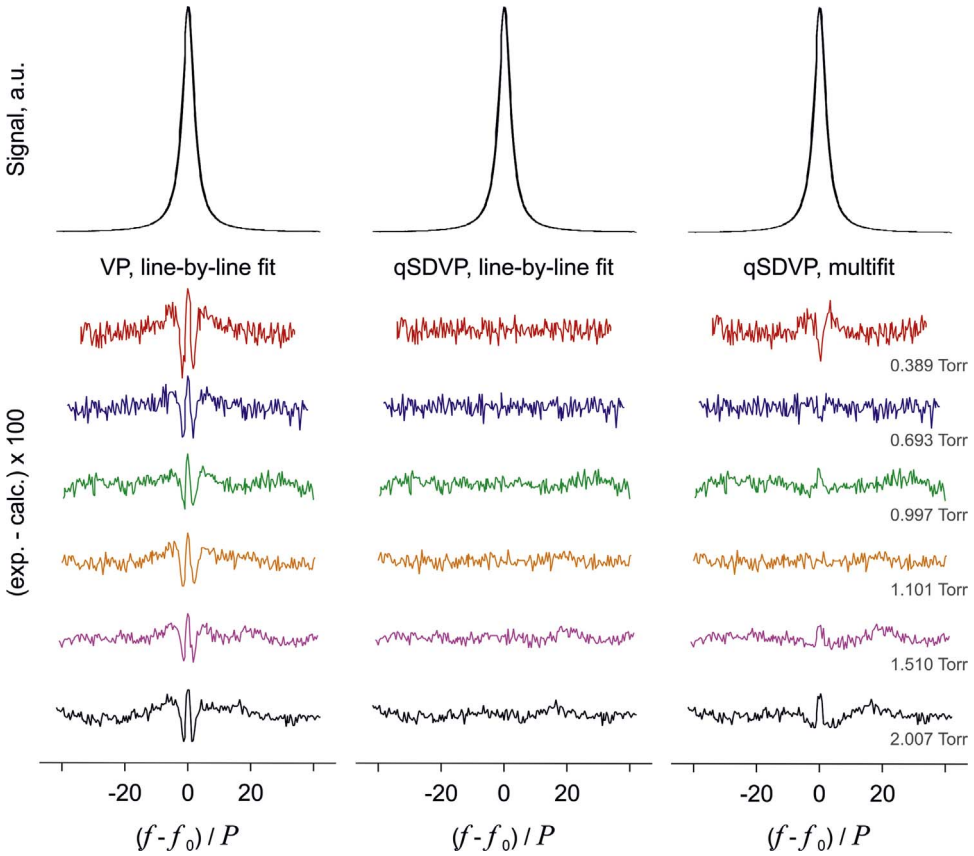

Fig. 5. (Color online) Experimental recordings (upper part) of the 118-GHz N = 1- oxygen line and zoomed in 100 times fit residuals (lower part) obtained using the VP and qSDVP line shape models and multispectrum and line-by-line analysis. Frequency scales (in MHz/Torr) correspond to frequency detuning from the line center (118750.332 MHz) normalized by the gas pressure.

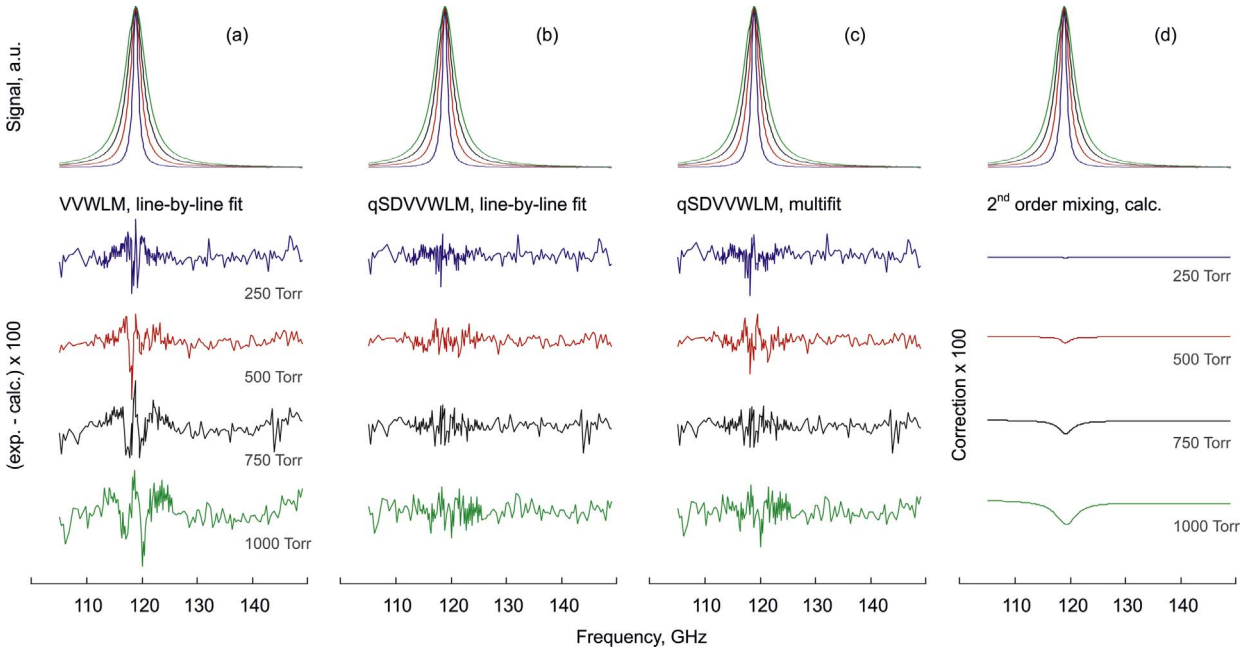

Fig. 6. (Color online) Experimental spectra ((a)-(d), upper part) and zoomed in 100 times fit residuals ((a)-(c), lower part) for the 118-GHz N = 1- oxygen line using VVWLM and qSDVVWLM line shape models. Model function, fitting method and corresponding pressure are presented in the figure. (d) Calculated contribution (x100) of the 2nd order line mixing at different pressures.

but we directly precalculated the contribution of the second-order terms using MPM values [41] and added it to the model function (5) together with the calculated contribution of the 60-GHz wing (see Fig. 4). The concentration of absorbing molecules (21% in MPM, 100% in experiment) was taken into account in the calculations. We didn't find any noticeable difference between residuals obtained with and without consideration of the second-order terms in the model or not, supporting our initial guess that the influence of the

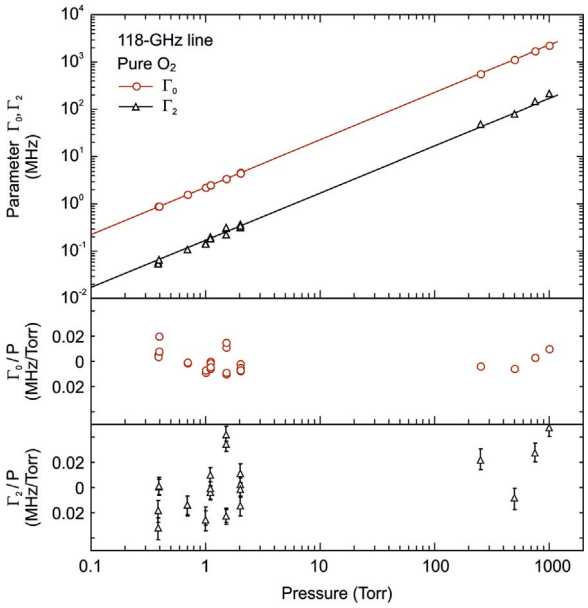

Fig. 7. (Color online) Upper part: Pressure dependence of Γ_0 (circles) and Γ_2 (triangles) of the 118-GHz N=1- oxygen line determined from the line-by-line fitting of the corresponding line profile (see text for details) to the low and high pressure spectra. Solid lines are results of linear approximation of the full set of experimental data which combines both high and low pressure data. Lower part: (exp-minus-calc) residuals of the upper plot normalized by pressure for figure clarity. Error bars are $\pm 1\sigma$ statistical uncertainty (they are less than point size for Γ_0 residuals).

second-order line-mixing approximation was insignificant in our spectra. However, all results presented in this paper were obtained by including precalculated second order line-mixing contribution in our model.

Results of line-by-line analysis of both low and high pressure spectra using speed dependent profiles are shown in Figs. 7–9. Excellent coincidence and linear growth of both Γ_0 and Γ_2 values obtained from low and high pressure spectra is demonstrated in Fig. 7. It proves that deviation of the 118-GHz oxygen line shape from the classical one observed in the wide (changing within four orders of magnitude) pressure range of our experiments is mainly caused by the speed dependent effect. The residuals of the linear approximation of the pressure dependences of Γ_0 and Γ_2 shown in the lower part of Fig. 7 demonstrate high precision and accuracy of the obtained data.

RAD spectrometer does not allow accurate measurement of line intensity, so it was determined only from the high pressure spectra

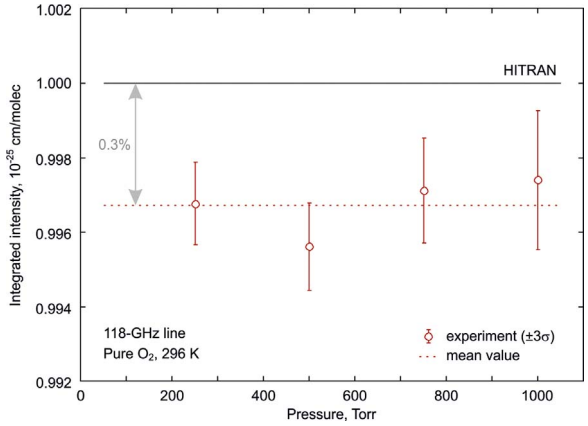

Fig. 8. (Color online) Measured integrated intensity (circles) of the 118-GHz oxygen line recalculated to 296 K and their mean value (dotted line). Error bars correspond to $\pm 3\sigma$ statistical uncertainty. Solid line is HITRAN's value.

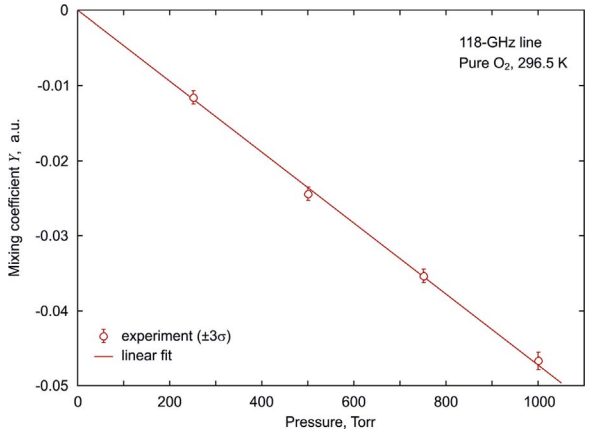

Fig. 9. (Color online) Measured line mixing parameter Y (circles) of the 118-GHz oxygen line obtained from the line-by-line fit of the qSDVVWLM profile to the high pressure spectra. Error bars correspond to $\pm 3\sigma$ statistical uncertainty. Solid line is linear approximation of the experimental data.

at 296.5 K. Then it was recalculated to 296 K (correction is about 0.3%) and compared (Fig. 8) with the value of $1.0 \cdot 10^{-25}$ cm/molec tabulated in the HITRAN database [44]. The relative difference between the experimental and HITRAN's values is only 0.3%, which may evidence high accuracy of intensities of all oxygen fine-structure lines tabulated in the database.

The line mixing effect cannot be studied using RAD spectrometer because its influence on line shape is negligible at pressures of about 1 Torr. The line mixing parameter Y determined from the high pressure spectra are plotted in Fig. 9 with $\pm 3\sigma$ statistical uncertainty. High accuracy and linearity of the data is worthy of notice.

The pressure shifting coefficient δ_0 and the unshifted central frequency f_0 were determined from weighted linear regression of the pressure dependence of experimental frequencies obtained from analysis of both low and high pressure spectra. The value of the inverse squared error was used as a weight. Our earlier studies [15,16,20,33] estimated this parameter to be less than ± 15 kHz/Torr (boundaries of the ordinate axis in Fig. 10). This very low value makes it almost impossible to see the manifestation of the speed-dependence of the shift Δ_2 considering our current signal-to-noise ratio so it was fixed to zero in the fitted models. High quality of the experimental data obtained in the current study in the wide pressure range allowed us to re-evaluate limits of the shifting parameter. Small positive bias of the experimental points (Fig. 10) is insignificant considering the experimental uncertainties. So we assume the shift of the 118-GHz oxygen line to be zero within ± 4.5 kHz/Torr (3σ of experimental points in Fig. 10). The central frequency found to be $f_0 = 118750.332(1)$ MHz

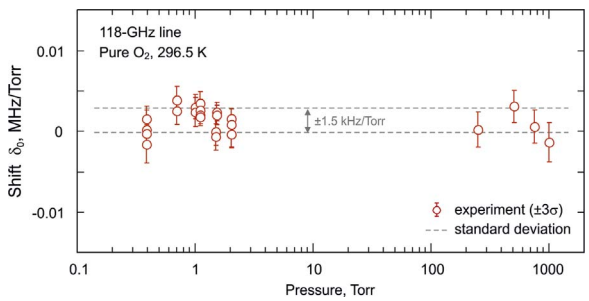

Fig. 10. (Color online) Measured shifting parameter Δ_0 of the 118-GHz N=1-oxygen line determined from the line-by-line fitting of the corresponding line profile to the low and high pressure spectra. Error bars correspond to $\pm 3\sigma$ statistical uncertainty. Dashed grey lines correspond to standard deviation of experimental points.

Table 1
Parameters of the 118-GHz N = 1- oxygen line at 23.5°C determined using multispectrum and line-by-line fitting approaches. The uncertainties in parentheses are 1σ statistical errors in the last quoted digit(s). γ_0, γ_2 and y – are normalized by pressure coefficients corresponding to Γ_0/P, Γ_2/P and Y/P.

Parameters	Multispectrum Fit	Line-by-line Fit
	RAD spectrometer (low pressures)	
γ_0 **(MHz/Torr)**	2.270(1)	2.269(2)
γ_2 **(MHz/Torr)**	0.161(3)	0.169(4)
	Resonator spectrometer (with 2nd order LM, high pressures)	
γ_0 **(MHz/Torr)**	2.272(1)	2.277(3)
γ_2 **(MHz/Torr)**	0.189(4)	0.203(11)
$y\times10^{-5}$ **(1/Torr)**	−4.71(3)	−4.71(4)
I_0 **x 10^{-25} (cm/molec)**	0.9933(8)	0.9935(6)

is in good agreement with the value 118750.33396 MHz [45] calculated from the global fit of the data known to that date in the wide range from microwave to UV.

Spectroscopic parameters for the 118-GHz N = 1- oxygen line obtained from analysis of low and high pressure spectra are listed in Table 1 together with their standard deviations. Both multispectrum and line-by-line approaches lead to similar (coinciding within $\pm 3\sigma$) results for the oxygen line parameters, proving that for both experimental data sets, baselines were taken into account correctly and correlation of parameters of the fitting model functions is minimal. The qSDVVWLM model used for high pressure data is more sophisticated than qSDVP because of a larger number of variable parameters. Stronger correlation between the qSDVVWLM model parameters leads to larger uncertainties and greater difference between multifit and line-by-line values.

The line shape parameter errors resulting from pressure and temperature uncertainty were estimated assuming a worst case scenario, i.e. $\pm 0.2\%$ or $\pm 0.25\%$ for pressure depending on gauge and ± 0.5°C for temperature. Relative temperature-related uncertainties of broadening and mixing parameters were evaluated using the common exponential law $X(T)=X(T_0)\cdot(T_0/T)^{n_X}$, where $X(T)$ is a parameter at temperature T, T_0 is a reference temperature. Temperature exponent $n_X = 0.765(11)$ [20] was assumed to be the same for broadening and mixing parameters (see, e.g. [18],). The uncertainty of n_X is negligible compared to the other error sources, so it was not taken into account. MPM definition of line intensity [13]

$$I_0(P,T) = a_1\cdot 10^{-6}\cdot P\cdot\left(\frac{T_0}{T}\right)^3\cdot\exp\left(a_2\cdot\left(1-\frac{T_0}{T}\right)\right)$$

was used for calculation of the error budget. Here, a_1 and a_2 are model parameters tabulated in MPM [13]. The error sources and the corresponding relative parameter errors contributing to the total uncertainty of the line shape parameters determination are presented in Table 2. Combined total uncertainty of each parameter was calculated as a squared root of the sum of squared errors.

Weighted averaging of all measured coefficients γ_0 and γ_2 from Table 1 gave the values of 2.271(7) MHz/Torr and 0.172(12) MHz/Torr, respectively, at 296.5 K. We recommend these values in combination with the line intensity $I_0 = 0.9934(36)\cdot 10^{-25}$ cm/molec and mixing coefficient $y = -4.71(3)\cdot 10^{-5}$ 1/Torr for further use for accurate modeling of line shape of the 118-GHz oxygen line. The errors in parentheses correspond to the combined total uncertainty of the parameter presented in Table 2.

It is interesting to compare parameters obtained by separate analysis of low and high pressure data. Thus, both pressure ranges give very comparable values for γ_0 and γ_2 parameters. Particularly,

Table 2
Error sources and corresponding relative parameter error (in %) contributing to the total uncertainty of the line shape parameters determination.

Parameter	Fit error, %	Pressure uncertainty, %	Temperature uncertainty, %	Total uncertainty,%
γ_0	0.1	0.25	0.13	0.30
γ_2	7	0.25	0.13	7.01
y	0.6	0.2	0.13	0.65
I_0	0.06	0.2	0.3	0.37

the maximum deviation for γ_0 between low and high pressure analysis is only 0.35%. For γ_2 the discrepancy is greater (maximum 15%) but again the determination of a speed-dependent collisional broadening parameter is more tricky at high pressure, and the agreement of the two analyses is very satisfactory considering the maximum pressure factor of about 3000 between the two pressure ranges (~ 0.4 – 1000 Torr). This allows us to validate collisional broadenings obtained in these two different pressure regimes. Further improvements of the resonator spectrometer SNR would certainly enable a better agreement for γ_2 value.

All previous studies of the 118-GHz oxygen line neglected the speed-dependence effect. For correct comparison of the current results with the previous values we fitted VP and VVWLM profiles to the low- and high-pressure data, respectively. The determined values of $\gamma=2.221(7)$ MHz/Torr and $y = -4.58(6)\cdot 10^{-5}$ 1/Torr recalculated to 300 K (errors are combined uncertainties) are in a very good agreement with the previous values of $\gamma(300\mathrm{K}) = 2.230$ (5) MHz/Torr and $y(300\ \mathrm{K}) = -4.7(1)\cdot 10^{-5}$ 1/Torr [18] (errors are statistical uncertainties) obtained using the VVWLM profile and can be considered as an improvement of the values used for traditional line shape profiles.

6. Discussion and conclusions

The sensitivity of our RAD and resonator spectrometers was improved, which enabled finding signal-to-noise ratio at spectra recordings of the order of a few thousands. The spectrometers were used to obtain the 118-GHz line recordings in two very different pressure ranges with high SNR and reproducibility. Both multispectrum and line-by-line approaches considered for the analysis of the two sets of data gave line shape parameter values in a very good agreement. The spectra analysis also enabled the first manifestation of the speed-dependence of the collisional broadening of the line, along with considerable refinement of other parameters, including collisional broadening, line-mixing and integrated intensity. A subroutine for calculating the qSDVVWLM profile (FORTRAN code) is presented in the Supplementary Material [46].

Good agreement between line parameters obtained from the low and high pressure recordings also permitted us to consider applications of the technique for further studies. In all previous studies as well as in our current study, the SD effect is considered through dependences of $\Gamma = \Gamma(v)$ and $\Delta = \Delta(v)$ and line mixing is modeled through the Rosenkranz approximation using mixing parameter Y which is supposed to be independent of the absorber speed. In other words, in this approach the diagonal elements of the relaxation matrix are speed-dependent, while the off-diagonal elements are speed-independent. However, to the best of our knowledge, no one ever modeled the effect of SD in off-diagonal terms (SDLM effect), which can be expressed as $Y = Y(v)$. At the present level of our experimental accuracy it is impossible to observe the speed-dependence of the line-mixing effect. However, further improvement of the quality of experimental spectra may open such an opportunity.

Acknowledgments

The work was partially supported by the RFBR (grants 15-02-7748, 15-02-07887, 15–45-02335) and by the Government of the Nizhny Novgorod region. The support under the State project No. 0035–2014-009 is acknowledged. The authors would like to thank J.-M. Hartmann for helpful discussions and P.W. Rosenkranz for informal review of the paper.

Appendix A. Supporting information

Supplementary data associated with this article can be found in the online version at http://dx.doi.org/10.1016/j.jqsrt.2017.03.043.

References

[1] Tretyakov MYu. Spectroscopy underlying microwave remote sensing of atmospheric water vapor. JMS 2016;328:7–26.
[2] Ali Ali DS, Rosenkranz PW, Staelin DH. Atmospheric sounding near 118 GHz. J Appl Meteorol 1980;19:1234–1238.
[3] Waters JW. The Earth Observing System Microwave Limb Sounder (EOS MLS) on the Aura satellite. IEEE Trans Geosci Remote Sens 2006;44:1075–1092.
[4] Artman JO, Gordon GP. Absorption of microwaves by oxygen in the millimeter wavelength region. Phys Rev 1954;96:1237–1245.
[5] Hill RJ. Water vapor-absorption line shape comparison using the 22-GHz line: the Van Vleck–Weisskopf shape affirmed. Radio Sci 1986;21:447–451.
[6] Schulze AE, Tolbert CW. Shape, intensity and pressure broadening of the 2.53-millimetre wave-length oxygen absorption line. Nature 1963;200:747–750.
[7] Gimmestad GG, Llewellyn-Jones DT, Gebbie HA. Millimetre wave oxygen attenuation measurements. JQSRT 1976;16:899–900.
[8] Setzer BJ, Pickett HM. Pressure broadening measurements of the 118.750 GHz oxygen transition. J Chem Phys 1977;67:340–343.
[9] Pickett HM, Cohen EA, Brinza DE. Pressure broadening and its implications for cosmic background measurements. Astrophys J 1981;248:L49–L51.
[10] Read WG, Hillig KW, Cohen EA, Pickett HM. The measurement of absolute absorption of millimeter radiation in gases: the absorption of CO and O_2. IEEE Trans Anten Propagat 1988;36:1136–1143.
[11] Smith EW. Absorption and dispersion in the O_2 microwave spectrum at atmospheric pressures. J Chem Phys 1981;74:6658–6673.
[12] Drouin BJ. Temperature dependent pressure induced linewidths of $^{16}O_2$ and $^{18}O^{16}O$ transitions in nitrogen, oxygen and air. JQSRT 2007;105:450–458.
[13] Liebe HJ, Rosenkranz PW, Hufford GA. Atmospheric 60 GHz oxygen spectrum: new laboratory measurement and line parameters. JQSRT 1992;48:629–643.
[14] Tretyakov MYu, Parshin VV, Shanin VN, Myasnikova SE, Koshelev MA, Krupnov AF. Real atmosphere laboratory measurement of the 118-GHz oxygen line: shape, shift, and broadening of the line. JMS 2001;208:110–112.
[15] Golubiatnikov GYu, Koshelev MA, Krupnov AF. Reinvestigation of pressure broadening parameters at 60-GHz band and single 118.75 GHz oxygen lines at room temperature. JMS 2003;222:191–197.
[16] Tretyakov MYu, Golubiatnikov GYu, Parshin VV, Koshelev MA, Myasnikova SE, Krupnov AF, Rosenkranz PW. Experimental Study of Line Mixing Coefficient for 118.75 Oxygen Line. JMS 2004;223:31–38.
[17] Tretyakov MYu, Koshelev MA, Koval IA, Parshin VV, Kukin LM, Fedoseev LI, Dryagin YuA, Andriyanov AF. Temperature dependence of pressure broadening of 1- oxygen line at 118.75 GHz. JMS. 2007;241:109–111.
[18] Makarov DS, Koval IA, Koshelev MA, Parshin VV, Tretyakov Myu. Collisional parameters of the 118 GHz oxygen line: temperature dependence. JMS 2008;252:242–243.
[19] Koshelev MA, Vilkov IN, Tretyakov MYu. Pressure broadening of oxygen fine structure lines by water. JQSRT 2015;154:24–27.
[20] Koshelev MA, Vilkov IN, Tretyakov MYu. Collisional broadening of oxygen fine structure lines: the impact of temperature. JQSRT 2016;169:91–95.
[21] Hartmann J-M, Boulet C, Robert D. Collisional Effects on Molecular Spectra. Laboratory Experiments and Models, Consequences for Applications.Amsterdam: Elsevier; 2008.
[22] Seleznev AF, Fedoseev GV, Koshelev MA, Tretyakov MYu. Shape of collision-broadened lines of carbon monoxide. JQSRT 2015;161:171–179.
[23] Priem D, Rohart F, Colmont J-M, Wlodarczak G, Bouanich J-P. Lineshape study of the J=3-2 rotational transition of CO perturbed by N_2 and O_2. J Mol Struct 2000;517-518:435–454.
[24] Koshelev MA, Tretyakov MYu, Rohart F, Bouanich J-P. Speed dependence of collisional relaxation in ground vibrational state of OCS: rotational behavior. J Chem Phys 2012;136:124316.
[25] Rohart F, Nguyen L, Buldyreva J, Colmont J-M, Wlodarczak G. Lineshapes of the 172 and 602 GHz rotational transitions of $HC^{15}N$. JMS 2007;246:213–227.
[26] Tran H, Bermejo D, Domenech J-L, Joubert P, Gamache RR, Hartmann J-M. Collisional parameters of H_2O lines: velocity effects on the line-shape. JQSRT 2007;108:126–145.
[27] Ngo NH, Tran H, Gamache RR, Bermejo D, Domenech JL. Influence of velocity effects on the shape of N_2 (and air) broadened H_2O lines revisited with classical molecular dynamics simulations. Chem Phys 2012;137:064302.
[28] Berman PR. Speed-dependent collisional width and shift parameters in spectral profiles. JQSRT 1972;12:1331–1342.
[29] Dicke RH. The effect of collisions on the Doppler width of spectral lines. Phys Rev 1953;89:472–473.
[30] Makarov DS, Tretyakov MYu, Boulet C. Line Mixing in the 60-GHz Atmospheric Oxygen Band: comparison of the MPM and ECS Model. JQSRT 2013;124:1–10.
[31] Tretyakov MYu, Koshelev MA, Makarov DS, Tonkov MV. Precise Measurements of Collision Parameters of Spectral Lines with a Spectrometer with Radio-acoustic Detection of Absorption in the Millimeter and Submillimeter Ranges. Instrum Exp Tech+ 2008;51:78–88.
[32] Tretyakov MYu, Krupnov AF, Koshelev MA, Makarov DS, Serov EA, Parshin VV. Resonator spectrometer for precise broadband investigations of atmospheric absorption in discrete lines and water vapor related continuum in millimeter wave range. Rev Sci Instr 2009;80:093106.
[33] Tretyakov MYu, Koshelev MA, Dorovskikh VV, Makarov DS, Rosenkranz PW. 60-GHz oxygen band: precise broadening and central frequencies of fine structure lines, absolute absorption profile at atmospheric pressure, revision of mixing coefficients. JMS 2005;231:1–14.
[34] Parshin VV, Serov EA, Bubnov GM, Vdovin VF, Koshelev MA, Tretyakov MYu. Cryogenic resonator complex. Radiophys Quantum Electron 2014;56:554–560.
[35] Tretyakov MYu, Parshin VV, Koshelev MA, Shanin VN, Myasnikova SE, Krupnov AF. Studies of 183 GHz water line: broadening and shifting by air, N2 and O2 and integral intensity measurements. JMS 2003;218:239–245.
[36] Krupnov AF, Tretyakov MYu, Parshin VV, Shanin VN, Myasnikova SE. Modern Millimeterwave Resonator Spectroscopy of Broad Lines. JMS 2000;202:107–115.
[37] Van Vleck JH, Weisskopf VF. On the Shape of Collision-Broadened Lines. Rev Mod Phys 1945;17:227–236.
[38] Rohart F, Mader H, Nicolaisen HW. Speed dependence of rotational relaxation induced by foreign gas collisions: studies on CH_3F by millimeter wave coherent transients. J Chem Phys 1994;101:6475.
[39] Rohart F, Ellendt A, Kaghat F, and Mäder H Self and Polar Foreign Gas Line Broadening and Frequency Shifting of CH_3F: Effect of the Speed Dependence Observed by Millimeter-Wave Coherent Transients. JMS;185:222-233.
[40] Rosenkranz PW. Shape of the 5 mm oxygen band in the atmosphere. IEEE Trans Antennas Propag 1975;23:498–506.
[41] Makarov DS, Tretyakov MYu, Rosenkranz PW. 60-GHz oxygen band: precise experimental profiles and extended absorption modeling in a wide temperature range. JQSRT 2011;112:1420–1428.
[42] Delahaye T, Reed Z, Maxwell S, Hodges JT, Sung K, Brown L, Benner C, Devi VM, Warneke T, Spietz P, Tran H. Precise methane absorption measurements in the 1.64 μm spectral region for the MERLIN mission. J Geophys Res Atmos 2016;121:7360–7370.
[43] Ngo NH, Lisak D, Tran H, Hartmann J-M. An isolated line-shape model to go beyond the Voigt profile in spectroscopic databases and radiative transfer codes. JQSRT 2013;129:89–100.
[44] Rothman LS, Gordon IE, Babikov Y, Barbe A, Benner C, Bernath PF, Birk M, Bizzocchi L, Boudon V, Brown LR, Campargue A, Chance K, Cohen EA, Coudert LH, Devi VM, Drouin BJ, Fayt A, Flaud J-M, Gamache RR, Harrison JJ, Hartmann J-M, Hill C, Hodges JT, Jacquemart D, Jolly A, Lamouroux J, Le Roy RJ, Li G, Long DA, Lyulin OM, Mackie CJ, Massie ST, Mikhailenko S, Muller HSP, Naumenko OV, Nikitin AV, Orphal J, Perevalov V, Perrin A, Polovtseva ER, Richard C, Smith MAH, Starikova E, Sung K, Tashkun S, Tennyson J, Toon GC, Tyuterev VG, Wagner G. The HITRAN2012 molecular spectroscopic database. JQSRT 2013;130:4–50.
[45] Yu Sh, Miller CE, Drouin BJ, Müller HS. High resolution spectral analysis of oxygen. I. Isotopically invariant Dunham fit for the $X^3\Sigma_g^-$, $a^1\Delta_g$, $b^1\Sigma_g^+$ states. J Chem Phys 2012;137:024304.
[46] See Supplementary Material for FORTRAN code subroutine for calculating the qSDVVWLM profile.